Ultrathin surface-attached hydrogel coating for potential reversible nanogluing of implants

Laura Finck[1], Valentin Hagemann[2], Nina Ehlert[2], Sebastian Polarz[2], Henning Menzel[1*]

[1] Institute for Technical Chemistry, Braunschweig University of Technology, Hagenring 30, 38106 Braunschweig, Germany.

[2] Institute of Inorganic Chemistry, Leibniz-University Hannover, Callinstrasse 9, 30167 Hannover, Germany.

* Corresponding author: E-Mail: h.menzel@tu-braunschweig.de, Tel.: +49 531 391-5361

Abstract

A multifunctional copolymer of N-(2-Hydroxypropyl)methacrylamide (HPMA) and a phosphonate-containing monomer was developed with the aim of applying a hydrogel coating to implant surfaces. For this purpose, a copolymer was prepared that could bind to the implant surface (e.g. titanium) via a phosphonate group. A photocrosslinkable group (phenyl azide) and hydrophilic groups were also incorporated to form a hydrogel. Coatings of these polymers produced by spin coating and subsequent photocrosslinking were characterised by laser ellipsometry, which gave controlled dry layer thicknesses in the range 40 to 140 nm. Furthermore, the swelling ability was investigated by in-situ ellipsometry in different aqueous media. According to these measurements, the coatings can swell up to three times the initial dry film thickness, depending on their crosslinker content. We also validate long-term stability under physiological conditions.

In addition, the hydrogel coatings can immobilise different types of silica nanoparticles (non-porous silica (15 nm), nanoporous silica (40 nm) and periodic mesoporous organosilica (100 nm), which makes them suitable for nanogluing. Preliminary tests have shown that a PDMA hydrogel can indeed adhere to the surface-bound hydrogels by way of nanoparticles.

Key words: surface-attached hydrogel, nanogluing, silica nanoparticles.

1 Introduction

Over the last few decades, there has been a great deal of research into implant coatings. Research is often aimed at developing antibacterial coatings or drug-delivery systems to prevent implant removal. However, sometimes removal of implants is unavoidable for a variety of reasons. This may be due to a persistent infection or malpositioned implant, for example in the case of dental implants [1]. In the development of implant materials, it is of great interest to make implants safer. In addition to preventing infection, gentle removal should also be considered. There has been little research on simplified implant removal, so there is a great deal of interest in addressing this research gap.

One of the main problems during removal of an implant is the serious damage caused to the surrounding tissue. Inserting a new implant becomes more complicated and sometimes even the functionality of the implant is reduced when too much tissue has been destroyed. The aim is to develop implant coatings that normally enables a good integration into the tissue, but facilitate the removal of an implant by an external trigger if necessary. Hydrogels are suitable for this application as their structure and mechanical properties are very similar to human tissue [2]. Implants that are coated with hydrogels can enhance the soft tissue integration of medical implants. An enhanced integration also has the advantage that it prevents bacterial infection and implant failure [3].

Based on the work of Leibler et al., it is known that non-porous silica nanoparticles can bond synthetic hydrogels to other hydrogels or to soft tissue [4]. This effect is known as nanogluing or nanobridging. The reason for such strong adhesion is the adsorption of polymer chains onto the nanoparticle surface. Under constraint, the adsorbed layers are able to reorganise, dissipate energy and prevent the propagation of interfacial cracks [4]. In addition, Kim et al. describe an increase in bond strength with porous silica particles and attribute the increase to a higher surface area of the particles compared to non-porous particles of the same diameter [5]. However, it is not only the surface area that influences the strength of nanogluing. The cross-linking density of the hydrogels also has an effect on the adhesion, since the nanoparticles have to be of a size comparable to the mesh size of the hydrogels [4]. Furthermore, the concentration of nanoparticles in the solution plays a role in the gluing strength of two connected hydrogels. The strongest gluing can be achieved when a monolayer of nanoparticles is in between the hydrogel layers [5].

This knowledge will be used to develop a biomedical system that generally allows good integration into the body, but if removal is required, facilitated removal of the implant should be possible after application of an external trigger. The external trigger can be heat. It has been shown that iron oxide nanoparticles can generate heat in an alternating magnetic field

(AMF) by hyperthermia. This heat is very localised on the surface of the nanoparticles and decreases within a few nanometres distance [6]. To combine the properties of heating in an AMF and nanogluing, this study will use core-shell nanoparticles with an iron oxide core and a shell. As silica nanoparticles are known to be biodegradable, another class of material will be used for the shell: periodic mesoporous organosilica [7]. This material has the advantage of being easily tunable by exchanging the organic bridges. These nanoparticles will be used together with a surface-attached hydrogel to create an on-demand reversible system for intentional implant removal without causing damage to the surrounding tissue (see Figure 1). Here, the surface-attached hydrogel and the tissue form a strong adhesion through adsorption on the surface of the nanoparticles (Figure 1a). In an AMF the nanoparticles can produce heat (Figure 1b), leading to the desorption of surface-attached hydrogel and tissue (Figure 1c). A gentle removal is then feasible.

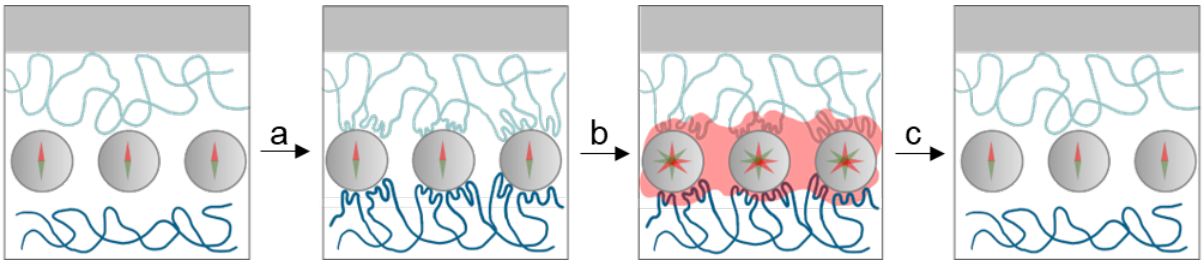

Figure 1: Schematic representation of the reversible nanoparticle adhesive. a) Adsorption of polymer strands onto the surface of the nanoparticles, b) AMF as trigger leads to heating of the nanoparticles, c) Polymer adsorption is released by high temperature.

This study focuses on the development of a suitable surface-attached hydrogel. A suitable polymer has to fulfil several requirements to act as a surface-attached hydrogel. Firstly, it must have a functional group to bind to an implant surface. A phosphonate group that can bind to implant materials such as titanium is suitable for this purpose [8]. In addition, a photocrosslinker is required to form surface-attached hydrogels. One suitable photocrosslinker is phenyl azide as it can form nitrenes under UV irradiation, which are a very reactive species, that can react in several ways to form crosslinks [9]. To achieve long-term stability, methacrylamides are used, which are known to be more stable against hydrolysis under physiological conditions than methacrylates [10]. N-(2-Hydroxypropyl)methacrylamide (HPMA) was selected as one of the monomers because it can be easily modified via its hydroxy group. Additionally, it is also known that PHPMA has a high biocompatibility and can form hydrogels by crosslinking. Woerly et al. were able to show that the PHPMA hydrogel promoted cell ingrowth and that there was no evidence of hydrogel degradation even after five months [11]. A copolymer of Diethyl-2-(methacrylamido) diethyl phosphonate (DMAAmEP) and HPMA was synthesized and modified post-polymerisation with phenyl azide. The resulting

copolymers were analyzed regarding coupling efficacy. The here prepared surface-attached hydrogel was investigated regarding its swelling ability and immobilization of different kind of nanoparticles.

2 Experimental

2.1 Materials

N-(2-Hydroxypropyl)methacrylamide (HPMA) Dimethylaminopyrridin (DMAP) and 4-azidobenzoic acid were supplied from TCI. Diethyl-2-(methacrylamido) diethyl phosphonate (DMAAmEP) was purchased from Specific polymers and the inhibitor was removed with Hydrochinon/Methyl ester inhibitor remover from Scipoly before usage. 1-Ethyl-3-(3-dimethylaminopropyl) carbodiimide hydrochloride (EDC HCl) and Dimethylformamid (DMF) were obtained from Carl Roth. 2,2′-Azobis(2-methylpropionitril) (AIBN) and phosphate buffered saline (PBS) tablets were supplied from Sigma Aldrich. Dichloromethane (DCM), dimethylsulfoxide (DMSO) and diethyl ether (Et_2O) were purchased from Fisher scientific. Spectra/Por®7 dialysis membranes with a molecular weight limit of 3500 kDa from Spectrum Labs were used for dialysis.

2.1.1 Poly-DMAAmEP-*co*-HPMA

1 molar solutions of the monomers in dry DMF were mixed in various ratios with a total volume of 2 mL in a screw cap test tube. Subsequently, 1 mol% AiBN was added. The reaction mixtures were purged with nitrogen for 2 min and sealed tightly. The reaction mixtures were shaken at 70 °C for 4.5 hours. The reaction was then stopped by immersion in ice. The polymers were precipitated in diethyl ether and then dried overnight in a vacuum. The polymer was then redissolved in MeOH, reprecipitated in diethyl ether and dried in vacuum. The polymer was obtained as white powder with a yield of 68% The experimentally obtained composition of the copolymer was calculated from the ratio of the integral of the 6 methylene protons of the phosphonate and the integral of the proton next to the OH-group of HPMA. Copolymerization parameters were calculated according to Kelen-Tüdos to be $r_{DMAAmEP}$ = 0.56 and r_{HPMA} = 0.74 (yield kept below 30%). In this report copolymers with a monomer ratio of 20:80 DMAAmEP to HPMA were used. DMF-SEC results in Mn = 23,390 g/mol (PDI = 1,9).

2.1.2 Poly-DMAAmEP-*co*-HPMA-Azide

Under a nitrogen atmosphere, a solution of EDC (0.63 - 0.158 eq) in dry DCM is added dropwise to a stirring solution of 4-azidobenzoic acid (0.125 - 1 eq; in the following always related to the OH group of HPMA) in dry DCM. The solution is stirred overnight at room temperature. The filtrate is added dropwise to a solution of the copolymer (1 eq OH groups) in DMSO. A solution of DMAP (1.05 eq) in DMSO is then added. The reaction solution is stirred

at 30 °C for 72 h. The modified polymer is dialyzed against 0.1 M NaCl solution and water. The solution is then freeze-dried. The experimentally obtained composition of the modified copolymer was calculated from the ratio of the integral of the proton in α-position to the ester and OH-group.

2.1.3 Nanoparticles

The non-porous Ludox nanoparticles were purchased from Sigma Aldrich and diluted to various concentrations.

2.1.3.1 Nanoporous Silica Nanoparticles

For the synthesis of nanoporous silica nanoparticles (NPSNP) 0.46 g diethanolamine and 6.32 g cetrimonium bromide (CTAB) were dissolved in a mixture of 26.8 mL ethanol and 150 mL water and heated up to 40 °C while stirring. After 30 minutes, 17.12 mL tetraethyl orthosilicate (TEOS) was added. The mixture was stirred for additional two hours, after which the nanoparticles were collected by centrifugation and washed twice with water and twice with ethanol and dried in vacuum. To remove CTAB, the particles were calcinated by heating to 550 °C over a period of ten hours with a heating rate of 1 °C per minute. This temperature was maintained for another five hours. The NPSNP have a size of 42 nm ± 4 nm as calculated by TEM (SI Figure 10). Nitrogen physisorption measurements resulted a BET surface of 1090 $m^2 \cdot g^{-1}$ and a total pore volume of 1.2 $cm^3 \cdot g^{-1}$, with an average pore size of 3.2 nm.

2.1.3.2 PMO@dSi@MNP

Oleic acid capped magnetite particles were synthesized by co-precipitation method published by Warwas et al. [12]. The synthesis procedure for the synthesis of PMO nanoparticles was conducted as described elsewhere [13]. The dense silica shell around the magnetite cores was build according to literature [14]. The synthesis of the PMO shell was carried out according to a modified procedure by Jahns et al. [15]. 40 mg of the previously synthesized Fe@dSiO2-NPs were dispersed in a mixture of 90 µL of Millipore water and 7.2 mL of ethanol for 10 minutes in an ultrasonic bath. Subsequently, 28 mL of millipore water, 1.4 mL (35.7 mmol) of a 25 wt% ammonium hydroxide solution, and 4.2 mL (0.5 mmol) of a 0.11 M CTAB solution were added. The CTAB solution was a 0.11 M solution in a 2:1 mixture of Millipore water and ethanol. After the addition, the vessel was shaken for two hours at 300 rpm at room temperature. Then, 176 µL (0.4 mmol) of 1,4-Bis(triethoxysilyl)benzene (BTEB) was added, and the vessel was shaken overnight at room temperature and 300 rpm. The next day, the vessel was heated at 80 °C in a convection oven for 24 hours. The particles were separated by centrifugation at 16 000 rpm and washed three times with ethanol centrifuged again, and dried under vacuum. The extraction of CTAB was carried out according to a modified

procedure by Lang et al. [16], by stirring the particles in 15 mL of ethanol with 0.17 g of ammonium nitrate for 1.5 hours at 80 °C. The extracted particles were then centrifuged, washed with ethanol, and dried under vacuum.

The average particle size is around 140± 15 nm, since there are aggregated particles with two or more dense Silica cores. While the dense Silica cores are around 50 nm, the PMO shell thickness is around 35 nm (SI Figure 10). Nitrogen physisorption measurements resulted a BET surface of 1190 $m^2 \cdot g^{-1}$ and a total pore volume of 1 $cm^3 \cdot g^{-1}$, with an average pore size of 3.5 nm.

2.1.4 Poly-Dimethylacrylamide (PDMA)

Poly-dimethylacrylamide was synthesized as described by Leibler et al. [4]. The hydrogels were prepared in a petri-dish and cut with a scalpel.

2.2 Methods

2.2.1 Coating procedure

The coating was carried out using a spin coater built in-house by the workshops of the Institutes of Technical, Physical and Theoretical Chemistry. Polymer solutions of concentration 10-30 mg/mL were prepared in MeOH. 65 µL of each of these solutions were placed on a polished titanium plate and spun for 30 seconds at 2000 rpm. The samples were stored in an oven at 120 °C for one night. UV irradiation was performed using a 365 nm UV lamp (UCUBE-365-100TM) from UWAVE (France) at an irradiance of 87 mW/cm^2 for 15 minutes. Finally, the platelets were washed in an ultrasonic bath with methanol and ultrapure water twice for 10 minutes each.

2.2.2 Ellipsometry

A multiscope from Optrel was used to determine the coating thicknesses. The measurements were processed using Optrel software 3.2. Measurements were carried out using an incidence angle of 70°. The surface of the coated substrates was scanned with 16 data points in a 4 × 4 matrix. Data evaluation was carried out using ELLI Version 3.2 from Optrel and a three-layer model (titanium, polymer, air) was used for the evaluation. The polymer was assumed to be homogenous. For the dry layer the refractive index of the polymer was kept in a range between 1.35 and 1.6 for modelling. The measurement setup was modified to measure the swelling properties in aqueous media. Quartz glass cuvettes immersed in the medium were attached to the laser and detector arm. Again, a three-layer system (titanium, polymer, water) was chosen for modelling the layer thickness in the swollen state. The polymer was assumed as

being homogenously swollen. For the swollen layers the refractive index for the polymer layer was kept close to the refractive index of water (1.33).

2.2.3 Scanning electron microscope (SEM)

SEM images were recorded on a Thermo scientific Helios G4 CX Dual Beam.

2.2.4 Gelpermeation chromatography

Molecular weight distributions were measured on a PSS SECcurity2 instrument equipped with a PSS GRAM column (Precolumn 10 µm, 8x50 mm, 2 main columns: 1000 A, 10 µm, 8x300 mm and 1000 A, 10 µm, 8x300 mm) in DMF containing LiBr (0.1 M) at a flow rate of 0.5 m/min at 40°C. The system was calibrated with narrow Polystyrene calibration standards.

2.2.5 UV-Vis spectroscopy

UV-Vis spectra were measured on a JascoV-630 (Pfungstadt, Germany) and used for determination of the degree of substitution (DS). For this purpose, a calibration with 4-azidobenzoic acid solution of different concentrations was used (ε=18,13059 L^2/mmol) and the calculation of the DS is possible with LAMBERT-BEER law.

2.2.6 zeta-potentials

The ζ-potentials of the nanoparticles used were determined on a Zetasizer NanoZS from Malvern (Kassel, Germany).

The ζ-potential of the coatings were measured on a SurPASS™ 3 from Anton Paar (Graz, Austria). The software used was SurPASS 3 software version 2.10.270.5111 release. Titanium grade 4 with the dimensions 10 mm x 20 mm x 2 mm was used as the substrate and prepared and coated in the same way as for the ellipsometry (vide supra). For the measurement, the samples were attached to the sample holders with double-sided adhesive tape. The gap size was adjusted to 100 µm in several rinsing steps with the aqueous 0.01 M KCl solution. The flow potential was measured with an Ag/AgCl electrode. The ζ-potential as a function of pH was determined in an aqueous solution of 0.01 M KCl.

2.2.7 Coating stability

The stability of the coatings was tested in two procedures. The first one is a Soxhlet extraction in methanol for 24 hours. The second one is done by immersion in phosphate buffered saline and 37 °C for 6 weeks to simulate physiological conditions.

2.2.8 Atomic force microscopy (AFM)

Topographical analysis of the polymer coatings was performed using the Veeco Multimode Nanoscope IIIa AFM (Santa Barbara, USA) in the Tapping Mode™. The software Gwyddion 2.65 was used to evaluate the data.

2.2.9 Transmission electron microscopy (TEM)

Transmission electron microscopy (TEM) was used to investigate the size and morphology of the particles. The measurements were performed on a Hitachi HT7800 @100 kV (Hitachi Ltd. Cooperation, Chiyoda, Japan). The nanoparticles were dispersed in ethanol using ultrasonication. A dispersion droplet of 10 µl was put on a holey carbon filmed copper grid (MicrotoNano, Harlem, Netherlands) and dried at room temperature. Images were recorded with a CMOS camera (14 bit 5120 x 3840 pixels emsis Xarosa) and acquired by RADIUS 2 imaging software. The particle sizes were determined using NIH ImageJ.

3 Results and discussion

Our approach to a surface-attached hydrogel coating involves the synthesis of a multifunctional copolymer. Besides N-(2-Hydroxypropyl)methacrylamide (HPMA), which is water soluble, the copolymer consists of a monomer with a phosphonate group which allows covalent immobilization on the titanium surfaces. In addition, a photocrosslinking group, phenyl azide, is incorporated into the polymer through partial Steglich esterification of hydroxy groups of the HPMA repeating unit (s. Figure 2). The films were prepared on titanium substrates by spin-coating a methanolic copolymer solution.

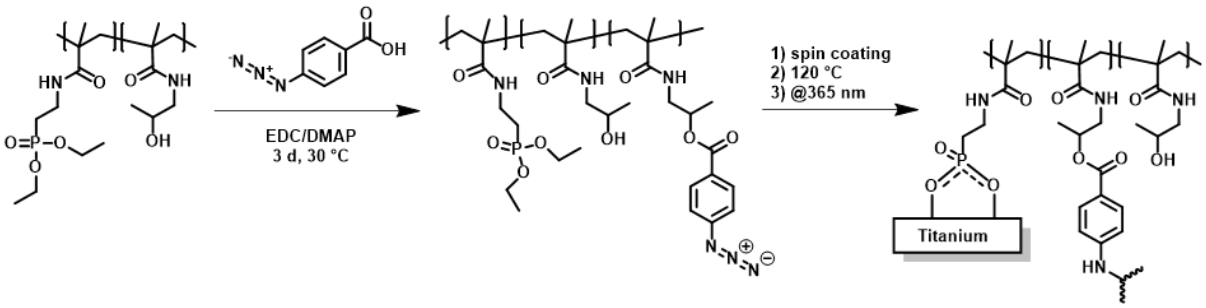

Figure 2: Synthetic route of surface-attached hydrogels on titanium.

3.1 Synthesis of the polymer

The two monomers, HPMA and DMAAmEP, were copolymerized in DMF by free-radical polymerization using AIBN as initiator. The r-parameters were determined by the Kelen-Tüdos method from ^{1}H-NMR spectra and gave $r_{DMAAmEP}$ = 0.56 and r_{HPMA} = 0.74. Therefore, the obtained r-parameter suggest a statistic distribution of the two monomers within the

copolymer. For further studies the content of the phosphonate moiety was kept at around 20%, as this content is enough for the covalent bonding to titanium [17,18]. The copolymerisation was carried out with approximately 70% yield.

The hydroxy group of the HPMA repeat unit can be used to introduce a photocrosslinking group. An attractive route to the formation of photoreactive phenyl azide copolymers is Steglich esterification. In our previous work we have shown that Steglich esterification of homopolymeric PHPMA with 3-(2-furyl)propionic acid via N,N'-dicyclohexylcarbodiimide (DCC) and Dimethylaminopyrridin (DMAP) works with a coupling efficacy between 50 and 60% [19]. We have transferred this reaction to the copolymer produced here, replacing DCC with 1-Ethyl-3-(3-dimethylaminopropyl)carbodiimide (EDC) due to the higher water solubility of the urea by-product and the slightly higher coupling efficiency (data not shown). The targeted crosslinker content is between 1 and 15%, which is a typical crosslinker content for hydrogel synthesis. The successful modification can be confirmed by ^{1}H-NMR (Figure 3) and UV-Vis spectra (SI Figure 11).

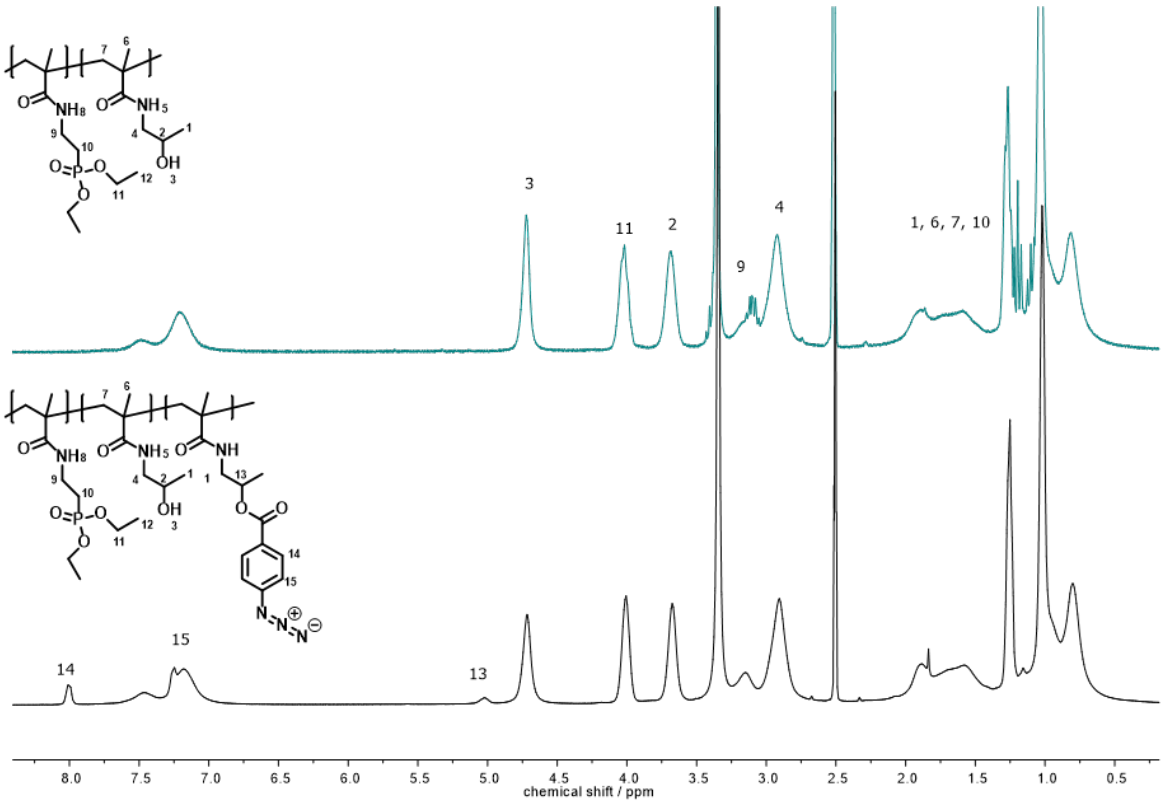

Figure 3: ^{1}H-NMR spectra of Poly-DMAAmEP-*co*-HPMA (top) and Poly-DMAAmEP-*co*-HPMA-Az (bottom).

In the ^{1}H-NMR new signals can be found belonging to the benzene ring of the phenyl azide (8.00 ppm and 7.25 ppm). In addition, the proton in α-position to the hydroxy group is shifted from 3.69 ppm to 5.03 ppm after esterification. Calculation of the degree of substitution (DS)

is possible for higher DS but becomes difficult for lower DS. Therefore, UV-Vis spectra were used to determine the DS using *Lambert-Beers* law (calibration line SI Figure 11). The desired crosslinker content could be achieved with this reaction, although only with a low coupling efficacy of below 30% (Table 1). The limiting reagent in this reaction is the coupling agent EDC, so the coupling efficacy is calculated as the quotient of DS and equivalents of EDC. The ratio of EDC to hydroxy group is critical in setting the DS, as one equivalent of EDC can functionalise exactly one repeat unit of HPMA. The reason for such a low CE may be that the polymer is sterically demanding, particularly due to the phosphonate bearing moieties.

Table 1: Overview of reached DS and their CE. DS was determined via UV-Vis

OH [eq]	Azide [eq]	EDC [eq]	DS [%]	CE [%]
1	1	0.63	14.4	22.9
1	0.75	0.473	13.2	27.9
1	0.5	0.315	8.8	27.9
1	0,35	0.221	4.4	20.0
1	0.25	0.158	2.8	17.7

These copolymers can then be used for rapid crosslinking on demand via UV light forming the highly reactive nitrene species which can react fast with NH- or CH-groups building a network [9].

3.2 Characterization of surface-attached hydrogels on titanium

Titanium is a commonly used implant material, e.g. for hip implants, due to its mechanical strength and good biocompatibility [20]. The surface of the polished titanium substrates is covered with a thin and stable titanium oxide layer, which allows the covalent attachment of phosphonate-containing polymers to the surface without further modification of the surface [8,17]. The copolymers were applied to the surface by spin coating from methanolic solutions. The samples were then annealed at 120 °C overnight to cleave some phosphonate ethyl esters and couple the polymers to the surface [8,21]. The samples were then irradiated at a wavelength of 365 nm to allow the azide to form cross-links via highly reactive nitrene species and cross-link the polymers in the coating [9,22]. This is followed by washing in an ultrasonic bath in methanol and Millipore water to remove unbound polymers. The coatings were characterised by ellipsometry and surface potential measurements. The long-term stability of the coatings was also tested.

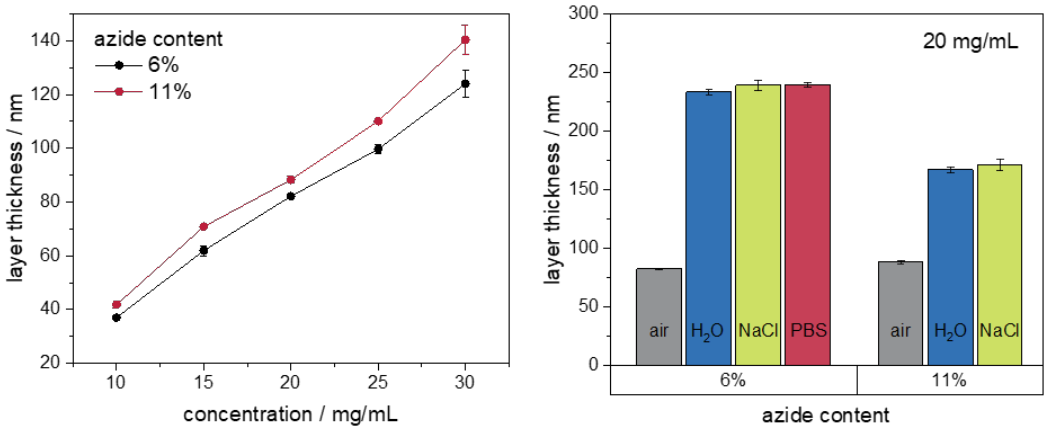

Figure 4: Dry layer thicknesses of the coatings with crosslinker content of 6% and 11% and various concentrations of the spin coating solution (left). Swollen layer thickness depending on the crosslinker content for 20 mg/mL coatings (right).

A series of tests with various concentrations of the coating solution were carried out with polymers containing 6% and 11% crosslinker and the resulting dry film thickness was measured by ellipsometry (see Figure 4, left). For both polymers there appears to be a linear relationship between concentration and film thickness, making it easy to achieve the desired film thickness over the concentration. Due to the relatively low molecular weights of around 25,000 g/mol, the viscosity does not seem to affect the spin coating process too much. Otherwise there would be a greater increase in film thickness at higher concentrations [23]. The difference between the thicknesses of the two polymers used is small and both show a higher coating inhomogeneity at the highest concentration of 30 mg/mL, as indicated by the larger error bar.

Additionally, measurements in a liquid cell were carried out to investigate the swelling ability of these coatings and thus forming surface-attached hydrogels. The model we used for the evaluation of the ellipsometric data includes the assumption that the coating is swollen homogeneously because after a few seconds the swollen layer thickness did not increase further. Different water-based media were tested as swelling medium: pure water, sodium chloride solution, and phosphate buffered saline (PBS). As seen from Figure 4, there is no difference in the swelling ability of the coatings in these media. The coating can swell up to 284% of their initial dry layer thickness in water for 6% azide containing polymers. For a higher azide content and thus higher crosslinking density, the coatings can only swell twice their dry thickness (189% for water). These results are as expected because hydrogels with a higher cross-linking degree are generally less able to swell. The swelling ratio is the same for the other concentrations tested.

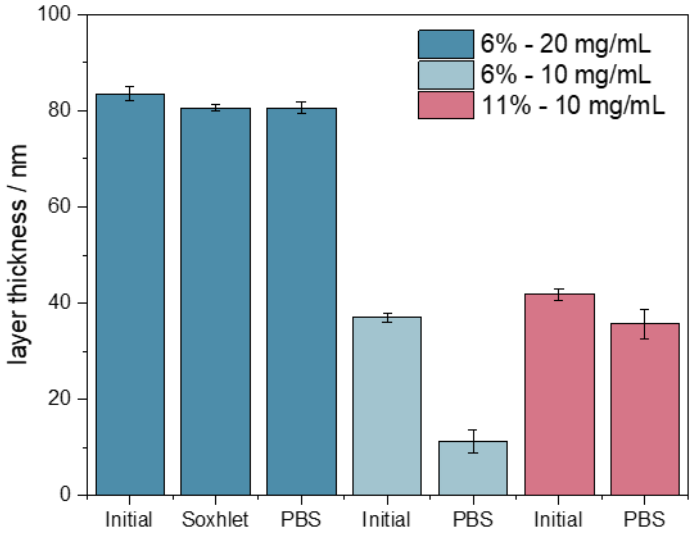

Figure 5: Long-term stability of the coatings on titanium.

Different coatings were tested for stability. Firstly, the coatings were subjected to a Soxhlet extraction in methanol to see if the coatings were stable under very harsh conditions. As can be seen in Figure 5, the coating thickness is constant after the extraction for 24 h. This result shows that after the washing process in the ultrasonic bath, all unbound polymer is washed out and the coatings are stable under these conditions. Another interesting question is whether the coatings are stable under body fluid conditions, in particular whether phosphate ions have an effect on stability. For this purpose, coated titanium plates were incubated in PBS buffer at pH 7.4 and at 37 °C. The coatings show different results depending on their initial dry layer thickness and crosslinker content. With an initial coating thickness of around 80 nm, the coating thickness is stable even after 6 weeks in PBS. In comparison, a lower initial film thickness with the same crosslinker content leads to a decrease in film thickness and is therefore not long-term stable. Increasing the crosslinker content from 6% to 11% reduces this effect, but still results in a slight decrease in film thickness. For further studies coatings with a layer thickness of around 80 nm will be used to provide samples with a high stability.

The pH dependent zeta potential measurements for the coatings were conducted to compare the zeta potential of the coatings with those of the nanoparticles, which will be used for the nanogluing experiments.

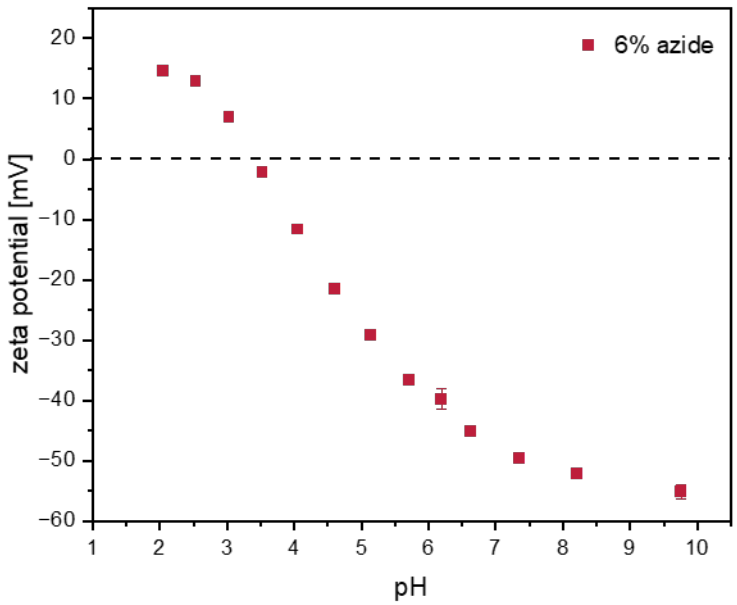

Figure 6: Zeta-potential between pH 2 and 10 of titanium coated with copolymer (20% DMAAmEP, 74% HPMA, 6% azide).

The surface potential is negative over a wide pH range. This phenomenon can be explained with the phosphonic esters being partially hydrolysed during the coating process including the annealing to bind to titanium [10]. However, not all of the resulting phosphonic acids bind to titanium. The free phosphonic acids can absorb or release protons depending on the pH value. The isoelectric point is between pH 3 and 4.

The HPMA-DMAAmEP copolymers can be applied to titanium and photocrosslinked via the phenyl azide groups, which were introduced in a polymer-analogous method. The coatings have a thickness that can be adjusted via the concentration of the spin coating solution, swell on contact with aqueous solutions and form hydrogels. The coatings are stable and have a negative surface charge in the physiological pH range.

3.3 Nanoparticle interactions and nanogluing

Silica nanoparticles can be adsorbed onto hydrogel surfaces [4]. The nanoparticles tested here include commercially available, non-porous silica nanoparticles (Ludox TM-50, 15 nm [4], ζ = -44.77 mV, pH 9), nano-porous silica nanoparticles (NPSNP, 42 nm, see SI Figure 10, ζ = -36.64 mV, pH 6) and periodic mesoporous silica nanoparticles (PMO, 100 nm (see SI Figure 10), ζ = -23.77 mV, pH 6). Ludox TM-50 nanoparticle solution was used without further treatment at a concentration of 50 wt%. The other nanoparticles were suspended in water at a concentration of 14 wt%. All Nanoparticles have a negative surface potential. To easily test

whether the nanoparticles could adsorb onto the surface-attached hydrogel coatings, a drop of nanoparticle solution was placed on the surface of the coating. After washing and soaking in water, the samples were imaged by scanning electron microscope (SEM).

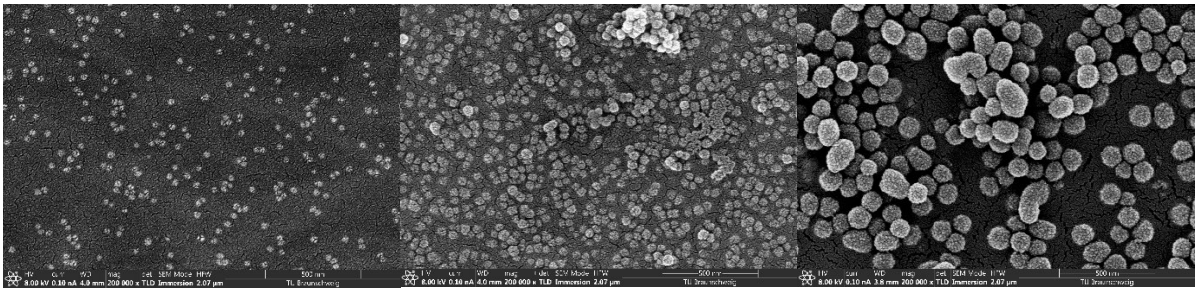

Figure 7: SEM images of the surface-attached hydrogel coating with different nanoparticles. Left: Ludox TM-50 (non-porous silica), middle: nanoporous silica (NPS), right: periodic mesoporous silica (PMO).

The SEM images show that all three types of nanoparticles are still present on the surface of the coatings after intensive washing. This finding suggests adsorption effects beyond electrostatic interactions as all nanoparticle solutions had a negative zeta potential at the given pH values, as did the coating. The Ludox TM-50 nanoparticles are well distributed over the entire surface and form a monolayer. The other two nanoparticles, on the other hand, show areas with monolayers as well as clusters, indicating some aggregation of the nanoparticles.

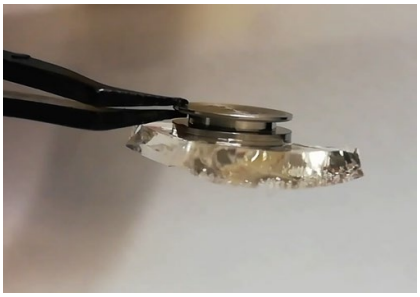

Figure 8: Adhesion of PDMA hydrogel through Ludox TM-50 nanoparticle.

Preliminary adhesion tests were conducted using the coating of Poly-DMAAmEP-co-HPMA-Az (DS=6%). A droplet of nanoparticle solution was applied to the surface and a piece of PDMA hydrogel was pressed onto the surface for 30 seconds. This procedure leads to some adhesion where the gel sticks to the coated sample and can hold its own weight. Figure 8 shows this phenomenon exemplarily for Ludox TM-50. This indicates that adhesion is possible with the right parameters. The bond strength needs to be further investigated in the future.

4. Conclusion

In this study DMAAmEP and HPMA were copolymerized and the r-parameters determined ($r_{DMAAmEP}$ = 0.56 and r_{HPMA} = 0.74) The copolymers were modified with phenyl azide as a photocrosslinking group. In this reaction degree of substitution could be adjusted via EDC and

DMAP concentrations. Coatings made of Poly-DMAAmEP-*co*-HPMA-Az can form ultrathin layers on titanium surfaces which subsequently can be photocrosslinked and have the ability to swell in aqueous media to form surface-attached hydrogels. The hydrogels show a negative surface potential at physiological pH. Furthermore, these coatings are stable under physiological conditions for at least six weeks. Their ability to interact with different kinds of silica nanoparticles was investigated showing an immobilization as established by SEM. The immobilisation of the nanoparticles cannot be attributed to opposing charges, as the zeta potentials of both the coating and the nanoparticles are negative. The results indicate that these coatings have the potential to act as a hydrogel in the nanogluing process with other hydrogels or tissues, as demonstrated by the initial adhesion tests.

Author contribution

Laura Finck: Writing – original draft, methodology, investigation, data curation, formal analysis, visualization, validation. **Valentin Hagemann:** methodology, investigation, data curation, formal analysis, validation. **Nina Ehlert:** Supervision, conceptualization, Writing – review and editing. **Sebastian Polarz:** Supervision, project administration, conceptualization, resources, Writing – review and editing. **Henning Menzel:** Funding acquisition, Supervision, project administration, conceptualization, Writing – review and editing, resources.

Funding sources

The work was funded by the Deutsche Forschungsgemeinschaft (DFG, German Research Foundation) -SFB/TRR-298-SIIRI-Project 426335750.

Use of AI-assisted technologies

During the preparation of this work the authors used DeepL.com in order to improve their English writing. After using this tool, the authors reviewed and edited the content as needed and take full responsibility for the content of the publication.

Acknowledgement

We would like to thank Maren Lindemann and Felix Künzel for contributing laboratory work to this study. We also thank Louise Niemeyer from the Institute for Particle Technology (iPAT) for conducting the SEM measurements. We dedicate this work to the memory of Prof. Peter Behrens†, whose invaluable contributions and dedication were essential to this research. His legacy and passion for knowledge will continue to inspire us.

References

[1] A. Solderer, A. Al-Jazrawi, P. Sahrmann, R. Jung, T. Attin, P.R. Schmidlin, Removal of failed dental implants revisited: Questions and answers, Clin. exp. dent. res 5 (2019) 712–724. https://doi.org/10.1002/cre2.234.

[2] A.S. Hoffman, Hydrogels for biomedical applications, Adv. Drug Delivery Rev. 64 (2012) 18–23. https://doi.org/10.1016/j.addr.2012.09.010.

[3] T.N. Dinh, S. Hou, S. Park, B.A. Shalek, K.J. Jeong, Gelatin Hydrogel Combined with Polydopamine Coating to Enhance Tissue Integration of Medical Implants, ACS Biomater. Sci. Eng. 4 (2018) 3471–3477. https://doi.org/10.1021/acsbiomaterials.8b00886.

[4] S. Rose, A. Prevoteau, P. Elzière, D. Hourdet, A. Marcellan, L. Leibler, Nanoparticle solutions as adhesives for gels and biological tissues, Nature 505 (2014) 382–385. https://doi.org/10.1038/nature12806.

[5] J.-H. Kim, H. Kim, Y. Choi, D.S. Lee, J. Kim, G.-R. Yi, Colloidal Mesoporous Silica Nanoparticles as Strong Adhesives for Hydrogels and Biological Tissues, ACS Appl. Mater. Interfaces 9 (2017) 31469–31477. https://doi.org/10.1021/acsami.7b09083.

[6] A. Riedinger, P. Guardia, A. Curcio, M.A. Garcia, R. Cingolani, L. Manna, T. Pellegrino, Subnanometer local temperature probing and remotely controlled drug release based on azo-functionalized iron oxide nanoparticles, Nano lett. 13 (2013) 2399–2406. https://doi.org/10.1021/nl400188q.

[7] J.G. Croissant, Y. Fatieiev, N.M. Khashab, Degradability and Clearance of Silicon, Organosilica, Silsesquioxane, Silica Mixed Oxide, and Mesoporous Silica Nanoparticles, Adv. Mater. 29 (2017). https://doi.org/10.1002/adma.201604634.

[8] N. Adden, L.J. Gamble, D.G. Castner, A. Hoffmann, G. Gross, H. Menzel, Synthesis and characterization of biocompatible polymer interlayers on titanium implant materials, Biomacromolecules 7 (2006) 2552–2559. https://doi.org/10.1021/bm060473j.

[9] S. Bräse, K. Banert, Organic azides: Syntheses and applications, Wiley, Chicester, 2010.

[10] S. Monge, G. David (Eds.), RSC Polymer Chemistry Series, Volume 11: Phosphorus-Based Polymers From Synthesis to Applications, Royal Society of Chemistry, Cambridge, GBR, 20140501.

[11] S. Woerly, E. Pinet, L. de Robertis, M. Bousmina, G. Laroche, T. Roitback, L. Vargová, E. Syková, Heterogeneous PHPMA hydrogels for tissue repair and axonal regeneration in the injured spinal cord, J. Biomat. Sci. Polym. Ed. 9 (1998) 681–711. https://doi.org/10.1163/156856298x00091.

[12] H.C. Janßen, D.P. Warwas, D. Dahlhaus, J. Meißner, P. Taptimthong, M. Kietzmann, P. Behrens, J. Reifenrath, N. Angrisani, In vitro and in vivo accumulation of magnetic nanoporous silica nanoparticles on implant materials with different magnetic properties, J. Nanobiotechnol. 16 (2018) 96. https://doi.org/10.1186/s12951-018-0422-6.

[13] V. Hagemann, L. Finck, T. Herrmann, H. Menzel, N. Ehlert, Core-Shell-Nanoparticles with Superparamagnetic Properties for Novel Applications as Biomaterials, Current directions biomed. eng. 9 (2023) 666–669. https://doi.org/10.1515/cdbme-2023-1167.

[14] J. Noh, S. Hong, C.-M. Yoon, S. Lee, J. Jang, Dual external field-responsive polyaniline-coated magnetite/silica nanoparticles for smart fluid applications, Chem. Commun. 53 (2017) 6645–6648. https://doi.org/10.1039/c7cc02197f.

[15] M. Jahns, D.P. Warwas, M.R. Krey, K. Nolte, S. König, M. Fröba, P. Behrens, Nanoporous hybrid core-shell nanoparticles for sequential release, J. Mater. Chem. B 8 (2020) 776–786. https://doi.org/10.1039/c9tb01846h.

[16] N. Lang, A. Tuel, A Fast and Efficient Ion-Exchange Procedure To Remove Surfactant Molecules from MCM-41 Materials, Chem. Mater. 16 (2004) 1961–1966. https://doi.org/10.1021/cm030633n.

[17] C. Pfaffenroth, A. Winkel, W. Dempwolf, L.J. Gamble, D.G. Castner, M. Stiesch, H. Menzel, Self-assembled antimicrobial and biocompatible copolymer films on titanium, Macromol. Biosci. 11 (2011) 1515–1525. https://doi.org/10.1002/mabi.201100124.

[18] M. Waßmann, A. Winkel, K. Haak, W. Dempwolf, M. Stiesch, H. Menzel, Influence of quaternization of ammonium on antibacterial activity and cytocompatibility of thin copolymer layers on titanium, J. Biomater. Sci., Polym. Ed. 27 (2016) 1507–1519. https://doi.org/10.1080/09205063.2016.1214001.

[19] L. Finck, V. Hagemann, P. Behrens, H. Menzel, Temperature-triggered liquefication of hydrogels for intentional implant removal, Current directions biomed. eng. 9 (2023) 158–161. https://doi.org/10.1515/cdbme-2023-1040.

[20] M. Geetha, A.K. Singh, R. Asokamani, A.K. Gogia, Ti based biomaterials, the ultimate choice for orthopaedic implants – A review, Prog. Mater. Sci. 54 (2009) 397–425. https://doi.org/10.1016/j.pmatsci.2008.06.004.

[21] G. Guerrero, P.H. Mutin, A. Vioux, Anchoring of Phosphonate and Phosphinate Coupling Molecules on Titania Particles, Chem. Mater. 13 (2001) 4367–4373. https://doi.org/10.1021/cm001253u.

[22] C. Hadler, K. Wissel, G. Brandes, W. Dempwolf, G. Reuter, T. Lenarz, H. Menzel, Photochemical coating of Kapton® with hydrophilic polymers for the improvement of neural implants, Mater. Sci. Eng., C 75 (2017) 286–296. https://doi.org/10.1016/j.msec.2017.02.020.

[23] B. Chollet, M. Li, E. Martwong, B. Bresson, C. Fretigny, P. Tabeling, Y. Tran, Multiscale Surface-Attached Hydrogel Thin Films with Tailored Architecture, ACS Appl. Mater. Interfaces 8 (2016) 11729–11738. https://doi.org/10.1021/acsami.6b00446.